HOPF CALCULATIONS IN DELAYED CAR-FOLLOWING MODELS

Gábor Stépán * **and Gábor Orosz** **

* *Department of Applied Mechanics, Budapest University of Technology and Economics, Budapest, H-1111, Hungary*
** *Mathematics Research Institute, University of Exeter, Laver Building, North Park Road, Exeter, EX4 4QE, UK*

Abstract: A nonlinear car-following model that includes the reaction-time delay of drivers is considered. When investigating the linear stability of the uniform flow solution, boundaries of Hopf bifurcations are determined in the parameter space. Crossing these boundaries, oscillations may appear corresponding to travelling wave solutions. Hopf normal form calculations prove robustly subcritical behavior which leads to bistability between the stable uniform traffic flow and the stop-and-go waves travelling against the flow of vehicles. Analogies with wheel shimmy dynamics and machine tool vibrations are presented.

Keywords: vehicular traffic, reaction-time delay, translational symmetry, subcritical Hopf bifurcation, bistability

1. INTRODUCTION

There are two important goals of traffic management when cars follow each other on a ring like M25 around London. The first goal is that the drivers travel with a speed close to their desired speed without hitting each other. The second goal is that the vehicles travel with the same constant velocity in a stable way, that is, the corresponding *uniform traffic flow* should be stable. In other words, this uniform traffic flow should survive smaller and/or larger perturbations, like a truck pulling out of its lane, without producing traffic jams on the road.

The first goal can be achieved with the help of the local control strategies of the drivers. This strategy involves a kind of optimal velocity function that describes how the drivers use the brake and the gas pedals to tune their velocities to the distances between their cars. The second goal is not always achieved just by means of the local control strategies of the drivers. When traffic jams develop as congestion waves travelling opposite to the flow of vehicles (Kerner, 1999), the stable uniform traffic flow may be achieved with appropriate traffic control that uses temporary speed limits by overhead gantries or may limit the number of cars entering the roads, etc.

In order to work out reasonable control strategies and to apply them properly, we must understand the nonlinear dynamics of the car-following systems. In this paper, we investigate a delayed car-following model and show the subcriticality of Hopf bifurcations related to the drivers' reaction-time delay. This explains how a stable uniform flow can coexist with a stable congestion wave, and why this nonlinear phenomenon has an essential role in future traffic management strategies.

The car-following model considered in this paper was first introduced in (Bando *et al.*, 1995) without the reaction-time delay of drivers where the system was investigated by numerical simulation. In (Gasser *et al.*, 2004) Hopf calculations have been carried out and numerical continuation technique, namely the package AUTO (Doedel *et al.*, 1997), was used to investigate the model, still without considering delay effects.

The reaction-time delay of drivers was first introduced in (Bando *et al.*, 1998), and its importance was shown by the study (Davis, 2003). In these papers numerical simulation was used to explore the nonlinear dynamics of the system. The first systematic global bifurcation analysis of the delayed model (Davis, 2003) was presented in (Orosz *et al.*, 2004) where numerical continuation technique, namely the package DDE-BIFTOOL

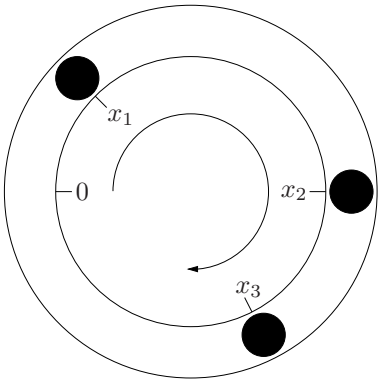

Fig. 1. Three vehicles on circular road.

(Engelborghs *et al.*, 2001), was used. The continuation results were extended to large numbers of cars in (Orosz *et al.*, 2005) where the dynamics of oscillations, belonging to different traffic patterns, were also analyzed. In this paper, we perform an analytical Hopf bifurcation calculation and determine the criticality of the bifurcation as a function of parameters for 3 vehicles on a ring in the presence of the drivers' reaction delay.

The appearance of the delay leads to delay differential equations (DDEs) and to infinite-dimensional phase spaces. The corresponding bifurcation theory of DDEs is available in (Hale and Verduyn Lunel, 1993). The infinite-dimensional dynamics make the bifurcation analysis more abstract. In particular, the stability analysis, the Jordan normal form, the center manifold reduction, and the Hopf normal form calculations require complicated algebraic formalism and algorithms, as shown in (Hassard *et al.*, 1981; Stépán, 1989; Campbell and Bélair, 1995; Orosz, 2004). In (Orosz and Stépán, 2004), the Hopf calculations have been extended for systems with translational symmetry. This translational symmetry is an essential property of car-following models. The method was demonstrated on the over-simplified case of 2 cars on a ring; see (Orosz and Stépán, 2004). Although this model already presented some of the most important properties of the nonlinear dynamics of the delayed models, the center manifold reduction still involved a simplification that cannot occur for systems with more than 2 cars.

In this study, these calculations are extended to 3 cars that increases the complexity of the center manifold reduction. This provides generalizable conclusions for the subcriticality of the bifurcations and its consequences for traffic jams and congestion waves. We prove that the delay makes the subcriticality of Hopf bifurcations robust, and bistability can occur. In the concluding part of the paper, we also present analogous nonlinear dynamics for shimmying wheels and that for cutting processes on machine tools.

2. MODELLING

Recall the basic features of the car-following model introduced and non-dimensionalized in (Orosz *et al.*, 2004) for n vehicles with periodic boundary conditions on the ring. As the number n of cars is increased, the significance of the periodic boundary conditions usually tends to become smaller. Still, in order to demonstrate the algebraic calculations in a manageable form, we only consider the lowest number of cars that does not lead to any trivial simplifications in the nonlinear analysis. Consequently, $n = 3$ vehicles are assumed to be distributed along a circular road of overall length L; see Fig. 1.

We assume that the 3 drivers have identical characteristics described by the scalar function V and the scalar parameter α. Considering that the 1st vehicle follows the 2nd vehicle, the 2nd follows the 3rd, and the 3rd follows the 1st, the equations of motion can be given as

$$\begin{aligned}
\ddot{x}_1(t) &= \alpha\big(\mathrm{V}\left(x_2(t-1) - x_1(t-1)\right) - \dot{x}_1(t)\big)\,,\\
\ddot{x}_2(t) &= \alpha\big(\mathrm{V}\left(x_3(t-1) - x_2(t-1)\right) - \dot{x}_2(t)\big)\,,\\
\ddot{x}_3(t) &= \alpha\big(\mathrm{V}\left(x_1(t-1) - x_3(t-1) + L\right) - \dot{x}_3(t)\big)\,,
\end{aligned} \tag{1}$$

where the position, the velocity, and the acceleration of the ith car ($i = 1, 2, 3$) are denoted by x_i, $\dot{x}_i$, and $\ddot{x}_i$, respectively; i.e., dot stands for time derivative. The so-called *optimal velocity function* $\mathrm{V}\colon \mathbb{R}^+ \to \mathbb{R}^+$ depends on the distance of the cars $h_i = x_{i+1} - x_i$, which is also called the *headway*. The argument of the headway contains the *reaction-time delay* of drivers which now is rescaled to 1. The dimensionless parameter $\alpha > 0$ is known as the *sensitivity*. The dimensionless equation (1) expresses that each driver approaches an optimal velocity, given by V, in an exponentially decaying way characterised by the *relaxation time* $1/\alpha > 0$. In the meantime, each driver reacts to its headway via a reaction-time delay 1.

One might, for example, consider the optimal velocity function to take the form

$$\mathrm{V}(h) = \begin{cases} 0\,, & \text{if} \quad 0 \le h \le 1\,,\\ v^0 \dfrac{(h-1)^3}{1+(h-1)^3}\,, & \text{if} \quad h > 1\,, \end{cases} \tag{2}$$

as already used in (Orosz *et al.*, 2004; Orosz *et al.*, 2005). This function is shown together with its derivatives in Fig. 2. The dimensionless parameter $v^0 = \max \mathrm{V}(h) > 0$ is called the *desired speed*, while the *jam headway*, up to which we have $\mathrm{V}(h) \equiv 0$, is now rescaled to 1.

Note that the time is rescaled with respect to the delay and the space is rescaled with respect to the jam headway. Consequently, the ratio of the dimensional time delay and relaxation time gives the dimensionless sensitivity α, while the dimensional desired speed times reaction delay over jam headway provides the dimensionless desired speed v^0; see details in (Orosz *et al.*, 2004).

3. HOPF BIFURCATIONS

The stationary motion of the vehicles, the so-called *uniform flow equilibrium* is described by

$$x_i^{\mathrm{eq}}(t) = v^*\, t + x_i^*\,, \quad \Rightarrow \quad \dot{x}_i^{\mathrm{eq}}(t) \equiv v^*\,, \quad i = 1, 2, 3\,, \tag{3}$$

where

$$x_2^* - x_1^* = x_3^* - x_2^* = x_1^* - x_3^* + L = L/3 := h^*\,, \tag{4}$$

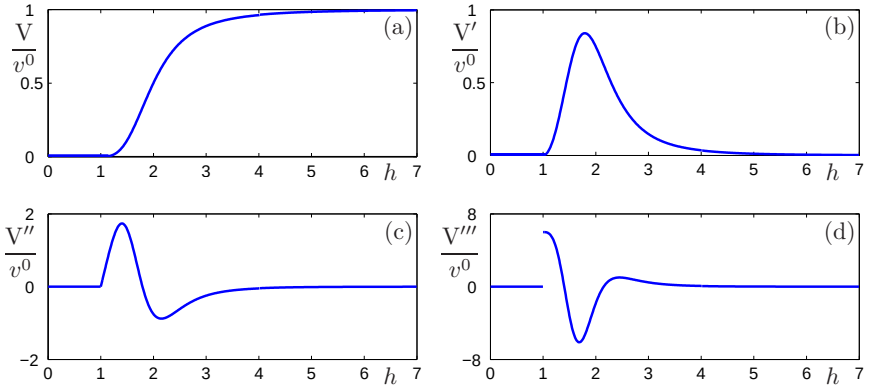

Fig. 2. The optimal velocity function (2) is shown in panel (a), and its derivatives are displayed in panels (b)–(d).

and

$$v^* = \mathrm{V}(h^*) < v^0\,. \tag{5}$$

Note that one of the constants x_i^* can be chosen arbitrarily due to the translational symmetry along the ring. Henceforward, we consider the *average headway* $h^* = L/3$ as a bifurcation parameter. Increasing h^* increases the length L of the ring, which involves scaling all headways h_i accordingly.

Let us define the perturbation of the uniform flow equilibrium by

$$x_i^{\mathrm{p}}(t) \colon = x_i(t) - x_i^{\mathrm{eq}}(t)\,, \quad i = 1,2,3\,. \tag{6}$$

Using Taylor series expansion of the optimal velocity function $\mathrm{V}(h)$ about $h = h^*(= L/3)$ up to third order of x_i^{p}, we can eliminate the zero-order terms

$$\begin{aligned}
\ddot{x}_1^{\mathrm{p}}(t) &= -\alpha\dot{x}_1^{\mathrm{p}}(t) \\
&\quad + \alpha \sum_{k=1,2,3} b_k(h^*)\big(x_2^{\mathrm{p}}(t-1) - x_1^{\mathrm{p}}(t-1)\big)^k\,, \\
\ddot{x}_2^{\mathrm{p}}(t) &= -\alpha\dot{x}_2^{\mathrm{p}}(t) \\
&\quad + \alpha \sum_{k=1,2,3} b_k(h^*)\big(x_3^{\mathrm{p}}(t-1) - x_2^{\mathrm{p}}(t-1)\big)^k\,, \\
\ddot{x}_3^{\mathrm{p}}(t) &= -\alpha\dot{x}_3^{\mathrm{p}}(t) \\
&\quad + \alpha \sum_{k=1,2,3} b_k(h^*)\big(x_1^{\mathrm{p}}(t-1) - x_3^{\mathrm{p}}(t-1)\big)^k\,,
\end{aligned} \tag{7}$$

where we introduce the notation

$$\begin{gathered}
b_1(h^*) = \mathrm{V}'(h^*)\,, \quad b_2(h^*) = \frac{1}{2}\mathrm{V}''(h^*)\,, \\
b_3(h^*) = \frac{1}{6}\mathrm{V}'''(h^*)\,.
\end{gathered} \tag{8}$$

At a critical bifurcation point h_{cr}^* the derivatives take the values $b_{1\mathrm{cr}} = \mathrm{V}'(h_{\mathrm{cr}}^*)$, $b_{2\mathrm{cr}} = \frac{1}{2}\mathrm{V}''(h_{\mathrm{cr}}^*)$, and $b_{3\mathrm{cr}} = \frac{1}{6}\mathrm{V}'''(h_{\mathrm{cr}}^*)$, where prime denotes differentiation with respect to the headway.

Introducing the notation

$$y := \mathrm{col}\,[\,\dot{x}_1^{\mathrm{p}} \;\; \dot{x}_2^{\mathrm{p}} \;\; \dot{x}_3^{\mathrm{p}} \;\; x_1^{\mathrm{p}} \;\; x_2^{\mathrm{p}} \;\; x_1^{\mathrm{p}}\,]\,, \tag{9}$$

equation (7) can be rewritten as

$$\dot{y}(t) = \mathrm{L}y(t) + \mathrm{R}(h^*)y(t-1) + F\big(y(t-1);h^*\big)\,, \tag{10}$$

where

$$\mathrm{L} \equiv \begin{bmatrix} -\alpha & 0 & 0 & 0 & 0 & 0 \\ 0 & -\alpha & 0 & 0 & 0 & 0 \\ 0 & 0 & -\alpha & 0 & 0 & 0 \\ 1 & 0 & 0 & 0 & 0 & 0 \\ 0 & 1 & 0 & 0 & 0 & 0 \\ 0 & 0 & 1 & 0 & 0 & 0 \end{bmatrix},$$

$$\mathrm{R}(h^*) = \alpha b_1(h^*) \begin{bmatrix} 0 & 0 & 0 & -1 & 1 & 0 \\ 0 & 0 & 0 & 0 & -1 & 1 \\ 0 & 0 & 0 & 1 & 0 & -1 \\ 0 & 0 & 0 & 0 & 0 & 0 \\ 0 & 0 & 0 & 0 & 0 & 0 \\ 0 & 0 & 0 & 0 & 0 & 0 \end{bmatrix}, \tag{11}$$

$$\begin{aligned}
&F\big(y(t-1);h^*\big) \\
&= \alpha \begin{bmatrix} \displaystyle\sum_{k=2,3} b_k(h^*)\big(y_5(t-1) - y_4(t-1)\big)^k \\ \displaystyle\sum_{k=2,3} b_k(h^*)\big(y_6(t-1) - y_5(t-1)\big)^k \\ \displaystyle\sum_{k=2,3} b_k(h^*)\big(y_4(t-1) - y_6(t-1)\big)^k \\ 0 \\ 0 \\ 0 \end{bmatrix}.
\end{aligned}$$

The steady state $y(t) \equiv 0$ of (10) corresponds to the uniform flow equilibrium (3) of the original system (1). Considering the linear part of (10) and using the trial solution $y(t) = S\mathrm{e}^{\lambda t}$ with $S \in \mathbb{C}^6$ and $\lambda \in \mathbb{C}$ we obtain

$$\big(\lambda - \mathrm{L} - \mathrm{R}(h^*)\mathrm{e}^{-\lambda}\big)S = 0\,. \tag{12}$$

which provides the characteristic equation

$$\begin{aligned}
&D\big(\lambda; b_1(h^*)\big) = \det\big(\lambda - \mathrm{L} - \mathrm{R}(h^*)\mathrm{e}^{-\lambda}\big) \\
&= \big(\lambda^2 + \alpha\lambda + \alpha b_1(h^*)\,\mathrm{e}^{-\lambda}\big)^3 - \big(\alpha b_1(h^*)\,\mathrm{e}^{-\lambda}\big)^3 = 0\,.
\end{aligned} \tag{13}$$

System (10) possesses a translational symmetry that is there exist a non-zero vector $S_0 \in \mathbb{R}$:

$$\begin{gathered}
\big(\mathrm{L} + \mathrm{R}(h^*)\big)S_0 = 0\,, \\
F\big(y(t-1) + S_0; h^*\big) = F\big(y(t-1); h^*\big)\,,
\end{gathered} \tag{14}$$

The first equation of (14) results in

$$\det\big(\mathrm{L} + \mathrm{R}(h^*)\big) = -D\big(0; b_1(h^*)\big) = 0\,, \tag{15}$$

i.e., there exist a zero characteristic root for any value of the parameter b_1, that is, for any value of the bifurcation parameter h^*:

$$\lambda_0(h^*) = 0\,. \tag{16}$$

Furthermore, by solving the first equation of (14) we have

$$S_0 = \mathrm{col}\,[\,0\;\;0\;\;0\;\;1\;\;1\;\;1\,]\,. \tag{17}$$

At a bifurcation point defined by $b_1 = b_{1\mathrm{cr}}$, i.e., by $h^* = h^*_{\mathrm{cr}}$, Hopf bifurcations may occur. Then there exists a complex conjugate pair of pure imaginary characteristic exponents

$$\lambda_{1,2}(h^*_{\mathrm{cr}}) = \pm \mathrm{i}\omega\,, \quad \omega \in \mathbb{R}^+\,, \tag{18}$$

which satisfies (13). To find the Hopf stability boundaries in the parameter space we substitute $\lambda_1 = \mathrm{i}\omega$ into (13). Separation of the real and imaginary parts gives

$$\begin{aligned} b_{1\mathrm{cr}} &= \frac{\omega}{\sqrt{3}\cos(\omega - \frac{\pi}{3})}\,, \\ \alpha &= -\omega\cot(\omega - \tfrac{\pi}{3})\,, \end{aligned} \tag{19}$$

where the resulting frequency $\omega \in (0, \frac{\pi}{3})$ is bounded.

Note that the function $b_1(h^*) = \mathrm{V}'(h^*)$ shown in Fig. 2(b) is non-monotonous, and so a $b_{1\mathrm{cr}}$ boundary typically leads either to two or to zero h^*_{cr} boundaries. In Fig. 3, the horizontal axis represents the uniform flow equilibrium and the Hopf bifurcation points are denoted by black stars. The equilibrium is unstable between the Hopf points (red dashed line) and stable otherwise (solid green lines).

Considering (12) at h^*_{cr}, substituting $\lambda_1(h^*_{\mathrm{cr}}) = \mathrm{i}\omega$ into that, and using (19) one obtains the eigenvector

$$S_1 = \mathrm{col}\,[\,\mathrm{e}^{\mathrm{i}\frac{2\pi}{3}}\;\;\mathrm{e}^{\mathrm{i}\frac{4\pi}{3}}\;\;\mathrm{e}^{\mathrm{i}2\pi}\;\;\tfrac{1}{\mathrm{i}\omega}\mathrm{e}^{\mathrm{i}\frac{2\pi}{3}}\;\;\tfrac{1}{\mathrm{i}\omega}\mathrm{e}^{\mathrm{i}\frac{4\pi}{3}}\;\;\tfrac{1}{\mathrm{i}\omega}\mathrm{e}^{\mathrm{i}2\pi}\,]\,. \tag{20}$$

By varying the parameter b_1, the necessary condition for Hopf bifurcation can be calculated by implicit differentiation of the characteristic equation (13):

$$\mathrm{Re}\left(\frac{\mathrm{d}\lambda_1(b_{1\mathrm{cr}})}{\mathrm{d}b_1}\right) = \frac{1}{b_{1\mathrm{cr}}}\,\underbrace{\frac{\left(\omega^2+\alpha^2+\alpha\right)}{\left(\frac{\alpha}{\omega}-\omega\right)^2+\left(2+\alpha\right)^2}}_{:=\,\mathcal{P}(\omega,\alpha)} > 0\,, \tag{21}$$

Since (21) is always positive, this Hopf condition is always satisfied. Now, using the chain rule and definition (8), condition (21) can be calculated further as the average headway h^* is varied to give

$$\begin{aligned} \mathrm{Re}\left(\lambda_1'(h^*_{\mathrm{cr}})\right) &= \mathrm{Re}\left(\frac{\mathrm{d}\lambda_1(b_{1\mathrm{cr}})}{\mathrm{d}b_1}\,b_1'(h^*_{\mathrm{cr}})\right) \\ &= \frac{2b_{2\mathrm{cr}}}{b_{1\mathrm{cr}}}\,\mathcal{P}(\omega,\alpha) \neq 0\,. \end{aligned} \tag{22}$$

This condition is fulfilled if and only if $b_{2\mathrm{cr}} \neq 0$, which is usually satisfied except at some special points; see Fig. 2(c).

At the critical parameter h^*_{cr}, (10) can be rewritten in operator differential equation form such that its linear and nonlinear parts contain the matrices $\mathrm{L}, \mathrm{R}(h^*_{\mathrm{cr}})$ and the function $F\big(y(t-1); h^*_{\mathrm{cr}}\big)$, respectively. Using (16,17), the translational symmetry related singularities can be eliminated as shown in (Orosz and Stépán, 2004). Then, with the help of (18,20), the system can be projected to the center manifold, where the essential dynamics take place. By taking into account the curvature of the center manifold, this essential dynamics can be identified. Finally, one can determine the so-called Poincaré-Lyapunov constant

$$\Delta = \frac{3}{8b_{1\mathrm{cr}}\omega^2}\mathcal{P}(\omega,\alpha)\left(6b_{3\mathrm{cr}} + \frac{(2b_{2\mathrm{cr}})^2}{b_{1\mathrm{cr}}}\mathcal{R}(\omega,\alpha)\right) \tag{23}$$

that determines the type of the bifurcation. The bifurcation is supercritical (i.e., the appearing oscillations are stable) for negative Δ, and it is subcritical (i.e., the appearing oscillations are unstable) for positive Δ. The rather complicated expression of $\mathcal{R}(\omega,\alpha)$ is not given here, but it is possible to prove that $\mathcal{R}(\omega,\alpha) > 0$ except for some large values of ω (that corresponds to fast oscillations in real traffic). Since $b_{1\mathrm{cr}}, b_{3\mathrm{cr}} > 0$ for realistic parameters, $\Delta > 0$ is obtained. This leads to robust subcriticality of the Hopf bifurcation.

Note that zero reaction-time delay results in $\mathcal{R}(\omega,\alpha) \equiv -1$ as shown in (Gasser *et al.*, 2004), while this ratio becomes positive for realistic reaction-time delay resulting in positive Δ. Consequently, the presence of the drivers' reaction-time delay has an essential role in the robustness of the subcritical nature of the Hopf bifurcation. This subcriticality explains how traffic waves can be formed even when the uniform flow equilibrium is stable, as detailed in the next section.

Using definition (8) and formulae (19,22,23), the amplitude A of the unstable oscillations is obtained in the form

$$\begin{aligned} A &= \sqrt{-\frac{\mathrm{Re}\left(\lambda_1'(h^*_{\mathrm{cr}})\right)}{\Delta}(h^* - h^*_{\mathrm{cr}})} \\ &= \omega\sqrt{-\frac{8}{3}\,\frac{\mathrm{V}''(h^*_{\mathrm{cr}})\,(h^* - h^*_{\mathrm{cr}})}{\mathrm{V}'''(h^*_{\mathrm{cr}}) + \frac{\left(\mathrm{V}''(h^*_{\mathrm{cr}})\right)^2}{\mathrm{V}'(h^*_{\mathrm{cr}})}\mathcal{R}(\omega,\alpha)}}\,. \end{aligned} \tag{24}$$

Close to the critical bifurcation parameter h^*_{cr} the unstable oscillations can be approximated by the first Fourier component:

$$y(t) = A\big(\mathrm{Re}(S_1)\cos(\omega t) - \mathrm{Im}(S_1)\sin(\omega t)\big)\,. \tag{25}$$

4. GLOBAL DYNAMICS

The unstable periodic motion given in (25) corresponds to a spatial wave formation in the traffic flow, which is actually unstable. Substituting (20) into (25) and using definitions (3,5,6,9), one can determine the velocity of the ith car as

$$\begin{aligned} \dot{x}_i(t) &= \dot{x}_i^{\mathrm{eq}}(t) + \dot{x}_i^{\mathrm{p}}(t) \\ &= \mathrm{V}(h^*) + A\cos\big(\tfrac{2\pi}{3}i + \omega t\big)\,, \quad i = 1,2,3\,. \end{aligned} \tag{26}$$

This describes a discrete wave travelling with the speed $\mathrm{V}(h^*) - \frac{3}{2\pi}h^*\omega$ which is negative for most parameter values, i.e., the wave propagates opposite to the car flow. These analytically estimated unstable periodic motions are presented in Fig. 3. The horizontal axis corresponds to the uniform

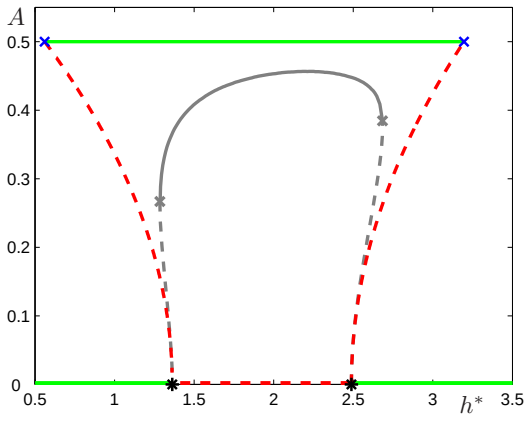

Fig. 3. The amplitude A of velocity oscillations as a function of the average headway parameter h^* for parameters $\alpha = 1.0$ and $v^0 = 1.0$. The horizontal axis ($A \equiv 0$) represents the uniform flow equilibrium and the analytical results are colored: green solid and red dashed curves represent stable and unstable branches, black stars stand for Hopf bifurcations, and blue crosses denote fold bifurcations. Grey curves correspond to numerical continuation results: solid and dashed curves refer to stable and unstable states, and grey crosses represent fold bifurcations.

flow equilibrium, that is, stable for small and large values of h^* (shown by green solid line) but unstable for intermediate values of h^* (shown by red dashed line) in accordance with formula (19) and Fig. 2(b). The equilibrium loses its stability at Hopf bifurcations that are marked by black stars. The emerging branches of the unstable periodic motions given by (24) are shown as red dashed curves.

Since the optimal velocity function is bounded so that $\mathrm{V} \in [0, v^0]$, an attractor must exist in our car-following system 'outside' the unstable limit cycle. Traffic experiments and also numerical simulations show that the external attractor is periodic again, and it includes travelling with speed close to the desired v^0, then decelerating, stopping for a while, and accelerating again close to the desired speed v^0. Since this heuristically constructed stable periodic motion has a peak-to-peak velocity value $2A \approx v^0 - 0$, the stable *stop-and-go oscillation* is represented by a horizontal green line at $A = v^0/2$ in Fig. 3 This *stop-and-go wave* also propagates against the traffic flow with about the same speed as the unstable traffic jam. The above simple heuristic construction reveals wide regions of bistability on both sides of the unstable equilibrium between the Hopf point (black star) and the heuristic fold point (blue cross) where the branches of stable and unstable oscillations meet. In such domains, depending on the initial condition, the system either tends to the uniform flow equilibrium or to the stop-and-go wave.

In order to check the reliability of the Poincaré-Lyapunov constant (23), the amplitude estimation (24) for the unstable periodic motion, the amplitude estimation $v^0/2$ for the heuristic stable stop-and-go motion, and the width of the resulting bistable parameter regime, we compared these analytical results with those obtained by the numerical continuation package DDE-BIFTOOL (Engelborghs *et al.*, 2001). In Fig. 3, the numerical continuation results are depicted in grey: grey solid curves represent stable oscillations while grey dashed curves represent unstable ones. The fold bifurcation points, where the branches of stable and unstable oscillations meet, are marked by grey crosses.

The comparison of the results shows that the analytical approximation of the unstable oscillations is quantitatively reliable in the vicinity of the Hopf bifurcation points. The heuristic amplitude $v^0/2$ of the stop-and-go oscillations is slightly larger than the numerically computed ones. The analytically suggested bistable region is larger than the computed one, since the third degree approximation is not able to predict fold bifurcations of periodic solutions. In order to find these fold bifurcation points, it is necessary to use numerical continuation techniques as presented in (Orosz *et al.*, 2005). Nevertheless, qualitatively the same structure is obtained by the two different techniques.

5. CONCLUSION AND ANALOGOUS NONLINEAR PHENOMENA

In the non-delayed model of (Bando *et al.*, 1995), subcriticality and bistablity occur only for extremely high values of the desired speed v^0, as it is demonstrated in (Gasser *et al.*, 2004). We proved that subcriticality and bistablity are robust features of the system due to the drivers' reaction-time delay, even for moderate values of the desired speed. This delay, which is smaller than the macroscopic time-scales of traffic flow, plays an essential role in this complex system because it changes the qualitative nonlinear dynamics of traffic.

Due to the subcriticality, stop-and-go traffic jams can develop for large enough perturbations even when the desired uniform flow is linearly stable. These perturbations can be caused, for example, by a slower vehicle (such as a lorry) joining the inner lane flow for a short time interval. In order to dissolve this undesired situation, an appropriate control can be applied using temporary speed limits given by overhead gantries that can lead the traffic back 'inside' the unstable travelling wave and then to reach the desired uniform flow.

The above described qualitative nonlinear dynamics has been explored in other physical applications where the presence of the unstable periodic motion causes similar problems in system design and control. In Fig. 4(a), the simplest mechanical model of wheel shimmy is shown (Stépán, 1998). The corresponding bifurcation diagram is displayed in Fig. 4(c) where one can identify subcritical Hopf bifurcations, unstable periodic motions, and also periodic (sometimes chaotic) attractors 'outside'. The appearance of the sliding of the wheel/ground contact point provides a similar nonlinearity as the stopping part of the optimal velocity function $\mathrm{V}(h)$ for $h \leq 1$. More details about shimmy can be found in (Takács, 2005).

In Fig. 4(c), the simplest model of machine tool vibration is shown for turning (Stépán, 1989). This dynamics involves time delay, shows subcritical Hopf bifurcations again as the angular velocity of

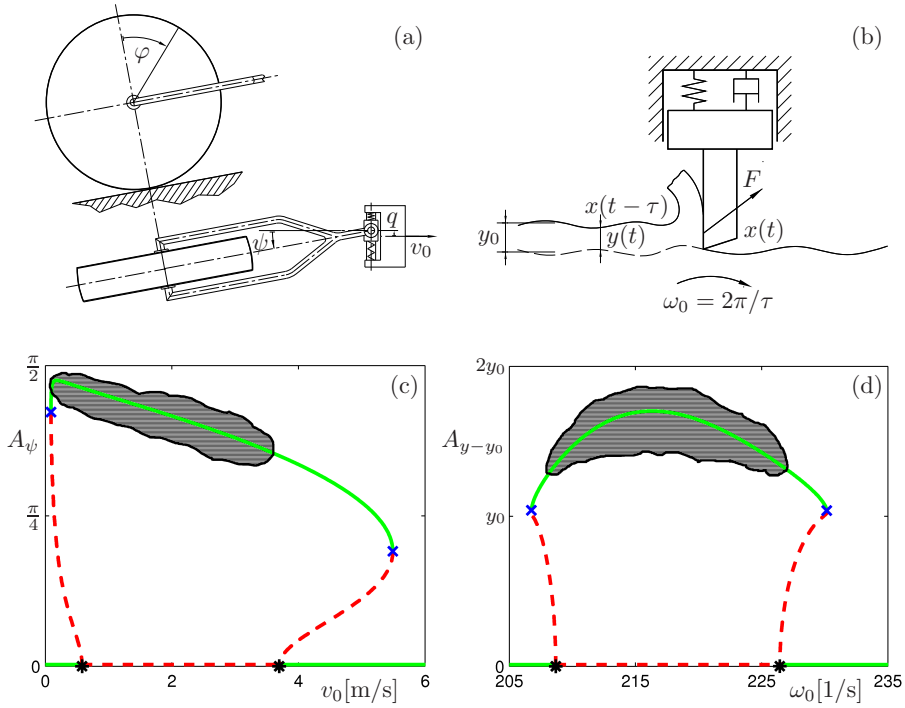

Fig. 4. Mechanical models of wheel shimmy and regenerative machine tool are shown in panels (a)–(b). The amplitude of caster angle as a function of the towing speed and the amplitude of chip thickness variation as a function of the angular velocity of rotation are depicted in panels (c)–(d) where the horizontal axis correspond to the equilibria. Stable and unstable states are represented by green solid and red dashed curves, respectively. Hopf bifurcations are shown by black stars and fold bifurcations by blue crosses. The shaded regions indicate the possibility of more complicated, e.g., chaotic dynamics.

rotation is varied as displayed in Fig. 4(d). Here the external periodic, sometimes chaotic attractor is provided by the nonlinearity originated in the loss of contact between the tool and the workpiece for $y(t) = y_0 + x(t-\tau) - x(t) \leq 0 \Rightarrow A_{y-y_0} \geq y_0$. This, is, again, analogous to the part $h \leq 1$ of the nonlinear optimal velocity function $\mathrm{V}(h)$ which prescribe that reversing of vehicles do not occur.

Acknowledgments: The authors greatly acknowledge the help and assistance of Dénes Takács on wheel Shimmy. This research was supported by the Hungarian National Science Foundation under grant no. OTKA T043368.

REFERENCES

Bando, M., K. Hasebe, A. Nakayama, A. Shibata and Y. Sugiyama (1995). Dynamical model of traffic congestion and numerical simulation. *Physical Review E* **51**(2), 1035–1042.

Bando, M., K. Hasebe, K. Nakanishi and A. Nakayama (1998). Analysis of optimal velocity model with explicit delay. *Physical Review E* **58**(5), 5429–5435.

Campbell, S. A. and J. Bélair (1995). Analytical and symbolically-assisted investigations of Hopf bifurcations in delay-differential equations. *Canadian Applied Mathematics Quarterly* **3**(2), 137–154.

Davis, L. C. (2003). Modification of the optimal velocity traffic model to include delay due to driver reaction time. *Physica A* **319**, 557–567.

Doedel, E. J., A. R. Champneys, T. F. Fairgrieve, Yu. A. Kuznetsov, B. Sandstede and X. Wang (1997). AUTO97. Department of Computer Science, Concordia University. `http://indy.cs.concordia.ca/auto/`.

. Engelborghs, K., T. Luzyanina and G. Samaey (2001). DDE-BIFTOOL Department of Computer Science, Katholieke Universiteit Leuven. `http://www.cs.kuleuven.ac.be/~koen/delay /ddebiftool.shtml`.

Gasser, I., G. Sirito and B. Werner (2004). Bifurcation analysis of a class of 'car-following' traffic models. *Physica D* **197**(3-4), 222–241.

Hale, J. K. and S. M. Verduyn Lunel (1993). *Introduction to Functional Differential Equations*. Vol. 99 of *Applied Mathematical Sciences*. Springer, New York.

Hassard, B. D., N. D. Kazarinoff and Y.-H. Wan (1981). *Theory and Applications of Hopf Bifurcation*. Vol. 41 of *London Mathematical Society Lecture Note Series*. Cambridge University Press, Cambridge.

Kerner, B. S. (1999). The physics of traffic. *Physics World* (August), 25–30.

Orosz, G. (2004). Hopf bifurcation calculations in delayed systems. *Periodica Polytechnica* **48**(2), 189–200.

Orosz, G. and G. Stépán (2004). Hopf bifurcation calculations in delayed systems with translational symmetry. *Journal of Nonlinear Science* **14**(6), 505–528.

Orosz, G., B. Krauskopf and R. E. Wilson (2005). Bifurcations and multiple traffic jams in a car-following model with reaction-time delay. *Physica D* **211**(3-4), 277–293.

Orosz, G., R. E. Wilson and B. Krauskopf (2004). Global bifurcation investigation of an optimal velocity traffic model with driver reaction time. *Physical Review E* **70**(2), 026207.

Stépán, G. (1989). *Retarded Dynamical Systems: Stability and Characteristic Functions*. Vol. 210 of *Pitman Research Notes in Mathematics*. Longman, Essex.

Stépán, G. (1998). Delay, nonlinear oscillations and shimmying wheels. In: *Applications of Nonlinear and Chaotic Dynamics in Mechanics* (F. C. Moon, Ed.). Kluwer Academic Publisher, Dordrecht. pp. 373–386.

Takács, D. (2005). Dynamics of rolling of elastic wheels. Master's thesis. Department of Applied Mechanics, Budapest University of Technology and Economics.